Journal of Power Sources 196 (2011) 3389–3394

Contents lists available at ScienceDirect

Journal of Power Sources

journal homepage: www.elsevier.com/locate/jpowsour

Effect of Ni nanoparticle distribution on hydrogen uptake in carbon nanotubes

Kuan-Yu Lin [a], Wen-Ta Tsai [a,*], Tsong-Jen Yang [b]

[a] Department of Materials Science and Engineering, National Cheng Kung University, 1 Ta-Hsueh Road, Tainan, Taiwan
[b] Department of Materials Science and Engineering, Feng Chia University, Taichung, Taiwan

ARTICLE INFO

Article history:
Received 26 January 2010
Received in revised form 7 April 2010
Accepted 8 April 2010
Available online 5 May 2010

Keywords:
Carbon nanotubes
Electroless plating
Ni nanoparticle
Hydrogen storage capacity

ABSTRACT

Ni decoration on carbon nanotubes (CNTs) performed by electroless nickel (EN) deposition is investigated. The effect of Ni particle distribution on hydrogen uptake of CNTs is also studied. The chemical composition, crystal structure and microstructure of the CNTs with or without Ni loading are characterized using an inductively coupled plasma spectrometer (ICP), X-ray diffraction meter (XRD) and transmission electron microscope (TEM) coupled with an energy dispersive spectroscope (EDS). The hydrogen uptake in CNTs with or without Ni loading is measured using a high-pressure microbalance at room temperature under a hydrogen pressure of 6.89 MPa. The experimental results show that fine and well-dispersed metallic Ni nanoparticles can be obtained by EN. The density and particle distribution depend on deposition temperature and time. An enhanced hydrogen storage capacity of CNTs can be obtained by Ni decoration, which provided a spillover reaction. The hydrogen storage capacity of the as-received CNTs was 0.39 wt.%. As much as 1.27 wt.% of hydrogen can be stored when uniformly distributed nano-sized Ni particles are formed on the surface of the CNTs. However, the beneficial effect is lost when the active sites for either physical or chemical adsorption are blocked by excessive Ni loading.

1. Introduction

The use of carbon materials such as carbon nanotubes (CNTs) as a hydrogen storage material has been of interest to both researchers and industry [1]. Hydrogen can be stored in carbon materials either by physi-sorption or chemi-sorption. It has been reported that the amount of physic-sorbed hydrogen in single wall carbon nanotubes (SWCNTs) can be as high as 2.5 wt.% [2] and that in multi-walled carbon nanotubes (MWCNTs) can be about 0.4 wt.% [3]. With the presence of catalysts, such as Pd, Pt, Ni, and Ru, hydrogen gas can be dissociated to hydrogen atoms due to the spillover effect [4,5], resulting in their chemi-sorption. Subsequently, the amount of hydrogen absorbed can be increased. For instance, Suttisawat et al. [6], have reported that the hydrogen adsorption capacity at room temperature and 65 bar was 0.125 and 0.1 wt.% for the Pd and V decorated CNTs, respectively, while the hydrogen uptake of the refined pristine CNTs was <0.01 wt.%. Kocabas et al. [7] reported that a hydrogen storage capacity of 1.66 wt.% could be attained if the CNTs were loaded with 10.1 wt.% Pd, 2.18 times higher than that of the raw materials. A much higher hydrogen storage capacity was reported by Mu et al. [8], who found that 4.5 wt.% of hydrogen could be stored by Pd-coated CNTs when the materials were charged in hydrogen gas at 10.7 MPa. Though the hydrogen storage capacity measured in different laboratories varies significantly, the beneficial effect of Pd-loading with regard to the hydrogen storage capacity of CNTs is quite obvious. Similar effects haves also been found when CNTs are decorated with other less expensive catalysts, such as V [6], Co [9] and Ni [10].

The loading of metallic particles on CNTs for use as catalysts, sensors, field emission and so on has been reported [11,12]. Several methods can be applied to decorate CNTs with metallic particles, including electrodepositition [13], chemical vapor deposition (CVD) [14], impregnation [15], and electroless plating [16]. The amount of particles and their distribution on the decorated CNTs varies with the deposition conditions. As far as hydrogen storage in carbon materials is concerned, Wang and Yang [17] indicated that the hydrogen capacity of active carbon decorated with 6 wt.% Ru was higher than those with 3 and 8 wt.% loadings. It seems that an optimum amount of catalyst may exist and that a peak hydrogen storage capacity can be obtained. Similar observations regarding the effects of Ni loading on CNTs preparing by impregnation method and their effect on hydrogen storage capacity has been reported elsewhere [18]. The abnormal dependence of catalyst loading on hydrogen storage behavior may be associated with the distribution on CNTs. However, the effect of particle distribution on the hydrogen storage behaviour has seldom been studied, especially for that loaded using an electroless deposition process. Therefore, in this investigation the distribution of particles formed by electroless Ni (EN) deposition on MWCNTs was studied, and the resulting effect on hydrogen capacity was explored.

* Corresponding author. Tel.: +886 6 2757575x62927; fax: +886 6 2754395.
E-mail address: wttsai@mail.ncku.edu.tw (W.-T. Tsai).

0378-7753/$ – see front matter © 2010 Elsevier B.V. All rights reserved.
doi:10.1016/j.jpowsour.2010.04.026

Table 1
Composition of EN plating solution.

Composition	Concentration
$Ni(CH_3COO)_2{\cdot}4H_2O$	84.5 g L^{-1}
$C_{10}H_{14}N_2Na_2O_8$	22.3 g L^{-1}
$C_2H_3NaO_3$	60 g L^{-1}
$N_2H_4{\cdot}H_2O$	50 mL L^{-1}

2. Experimental procedures

Commercial CNTs of 96 wt.% purity, 10–40 nm in diameter, and 5–20 μm in length, supplied by CNT Co., Ltd., Korea, were used in this study. The EN deposition was conducted following three steps: sensitization, activation and electroless deposition. Sensitization of CNTs was accomplished by stirring and dispersing the CNTs in a solution of 7 g $SnCl_2$ + 9 g HCl + 100 mL H_2O for 10 min. After complete washing in de-ionized water, the sensitized CNTs were further activated in an aqueous solution of 0.25 g $PdCl_2$ + 3 g HCl + 1 L H_2O for another 10 min. The ratios of solution volume to CNT weight (V/W) for both sensitization and activation processes were all adjusted at 2 L g^{-1}. The activated CNTs were then completely washed in de-ionized water prior to being placed in an EN plating bath. The composition of the EN bath, as shown in Table 1, was composed of 84.5 g L^{-1} $Ni(CH_3COO)_2{\cdot}4H_2O$ + 50 mL L^{-1} $N_2H_4{\cdot}H_2O$ + 22.3 g L^{-1} $C_{10}H_{14}N_2Na_2O_8$ (EDTA·2Na) + 60 g L^{-1} $C_2H_3NaO_3$, with a pH of 10.5. The EN plating was conducted at different temperatures (5–55 °C) for various periods of time (5–60 min). The V/W ratio of the EN bath was also controlled at 2 L g^{-1}. After EN coating, the CNTs were washed with de-ionized water and finally rinsed with ethanol for subsequent material characterization.

The amount of Ni coated onto CNTs was measured using an ICP spectrometer. The samples for ICP spectroscopy were prepared by dissolving the EN coated CNTs in 3.1 M HNO_3 solution with a known volume for 2 h when the Ni coating was completely dissolved. The solution was diluted to the order of 200 ppm before ICP spectroscopy. The identification of Ni coating and its crystallinity were also analyzed by XRD. The microstructure of CNTs with and without EN coating was characterized by a TEM. The samples for TEM analysis were prepared by dispersing CNTs in an anhydrous alcohol solution with super sonic vibration. A drop of the suspension fluid was then loaded and dried on a carbon coated copper grid for subsequent TEM analysis. The TEM analysis was performed using a high resolution TEM (HR-TEM) with a beam energy of 200 kV. The Ni particle distribution on CNT substrate was determined by measuring the particle size of more than 200 particles from TEM images, following the method described by Li et al. [19].

The hydrogen storage capacities of the as-received and the Ni-decorated CNTs were evaluated with a high-pressure microbalance (or thermal gravimetric analyzer, TGA) with a sensitivity of 10 μg. The weight of each sample was about 50 mg. The sample was first degassed at 300 °C for 2 h in a vacuum. After cooling down to room temperature, high purity hydrogen gas was introduced into the chamber up to 6.89 MPa. The weight change of the sample was recorded after 2 h when the microbalance reached a steady state. Calibrations were conducted to ensure the accuracy of weight change measurement using a high-pressure microbalance. The detailed procedure can be found elsewhere [20,21]. After hydrogen charging, the sample was degassed with the same condition mentioned above to release the absorbed hydrogen. Then, it was charged again for hydrogen storage capacity measurement. The above processes were repeated a few times for each sample to ensure the reversibility of charging and discharging reactions.

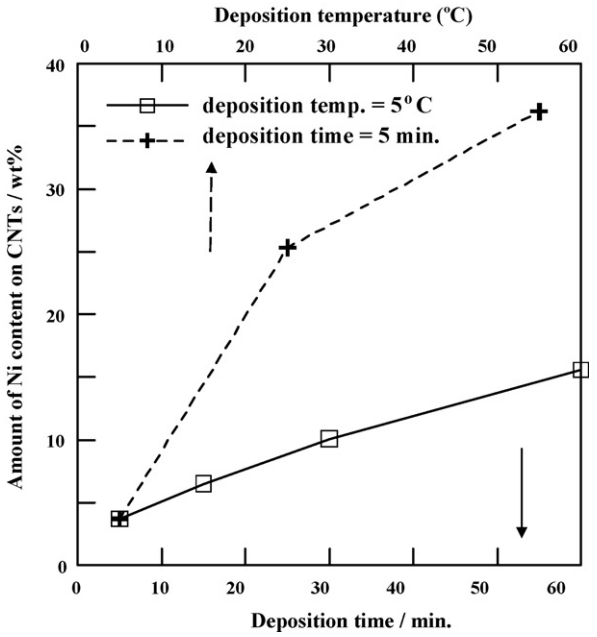

Fig. 1. Effects of deposition time and temperature on the amount of Ni deposited onto CNTs.

3. Results and discussion

The use of hydrazine (N_2H_4) as the reducing agent gave rise to the formation of pure Ni deposition. By dissolving the EN treated CNTs in nitric acid, the amount of Ni deposited could be determined by employing ICP spectroscopy. Fig. 1 shows the effects of temperature and deposition time on the amount of Ni deposited on the CNTs. When EN was conducted at 5 °C, the amount of Ni increased almost linearly with increasing deposition time, as demonstrated in Fig. 1. By controlling the deposition time at 5 min, the amount of Ni coated on the CNTs increased with increasing temperature, also shown in Fig. 1. Clearly the EN process can be successfully applied to deposit Ni on CNTs. As shown in Fig. 1, the effect of temperature on the amount of Ni deposition was much more pronounced than that of deposition time.

The XRD patterns of CNTs with and without EN coating were determined, as shown in Fig. 2. Curve *a* in Fig. 2 shows the XRD pattern of the as-received CNTs. Two broad peaks at 26.6° and 43.4° corresponding to the (0 0 2) and (1 0 1) planes of the HCP crystal structure of the fine CNTs were observed. Changes in the XRD patterns were observed if the CNTs were treated with EN at different temperatures and for various periods of time. Curve *b* in Fig. 2 shows the pattern for CNTs with Ni deposition at 5 °C for 30 min. The intensities of (0 0 2) and (1 0 1) for CNTs diminished slightly, as compared with curve *a*, while a small peak at 44.3° for (1 1 1) diffraction of FCC Ni appeared. By prolonging the deposition time to 60 min at 5 °C, the XRD pattern did not vary appreciably. The XRD patterns of Ni-coated CNTs are displayed in curve *c* when the deposition was performed at 25 °C for 5 min. As revealed in this pattern, a substantial increase in the intensity of the (1 1 1) peak for FCC Ni is observed, indicating a great amount of Ni deposition. As the deposition temperature was increased to 55 °C, with 5 min deposition time, the peak intensity of (1 1 1) for FCC Ni continued to increase, while that of (0 0 2) for HCP CNT decreased indicating the increasing amount of Ni deposition. The change in the intensity of (1 1 1) for FCC Ni, as revealed in Fig. 2, indicates that deposition temperature is more important than deposition time, as far as the amount of Ni deposition is concerned. Moreover, the broad peak of (1 1 1) for FCC Ni, as demonstrated in Fig. 2, indicates that the deposited Ni had very

fine grain size, as confirmed by TEM analysis, to be described later. The dependence of the deposited mass of pure Ni on temperature and time, as found in this investigation, is similar to that found for Ni–P deposits [22].

The appearance and distribution of Ni particles coated on CNTs were examined by TEM. Fig. 3 shows the micrograph of a CNT with EN coating conducted at 5 °C for 5 min. The multi-walled CNT displayed in Fig. 3(a) has an inner diameter and an outer diameter ranging from 5–8 to 12–15 nm, respectively. The dark spots are Ni particles deposited from the EN bath. The sizes of these particles are less than 4 nm, and the Ni peaks appearing in the EDS spectrum shown in Fig. 3(b) confirm their presence on CNTs. The subsequent TEM lattice image analysis, as will be described later further confirmed that Ni in metallic form was actually present on the CNTs.

At 5 °C, the number of Ni particles deposited on CNTs increases with deposition time. The TEM micrographs shown in Fig. 4 reveal that a higher density of Ni particles on CNTs was found when the deposition time was increased to 30 or 60 min, as compared with that shown in Fig. 3(a) with a deposition time of 5 min. It is noted, however, the particle size did not vary appreciably by increasing the deposition time from 30 to 60 min. These results suggest that progressive nucleation occurs at temperature as low as 5 °C, meanwhile the particle growth rate is very low, so that its size does not increase appreciably. At a higher magnification, the lattice image of Ni particles on the CNTs can be clearly seen, as demonstrated in the insets of Fig. 4(a) and (b). The d-spacing for the (1 1 1) plane of Ni particles is 2.049 Å, in agreement with that for the Ni formed by an impregnation process [23].

The particle size distribution of Ni deposited at 5 °C for 5, 30 and 60 min is shown in Fig. 5. The histogram shown in Fig. 5 is made by measuring the size in the longest direction of each particle from the TEM micrograph and counting the number of particles of a specific size. More than 200 particles are included for particle size distribution analysis. From the TEM images shown in Figs. 3 and 4, it can be seen that the number of Ni particles increased with increasing deposition time when EN was conducted at 5 °C. However, the histogram shown in Fig. 5 indicates that the mean particle size is about 2.3 nm for EN performed at 5 °C, which is almost independent of deposition time.

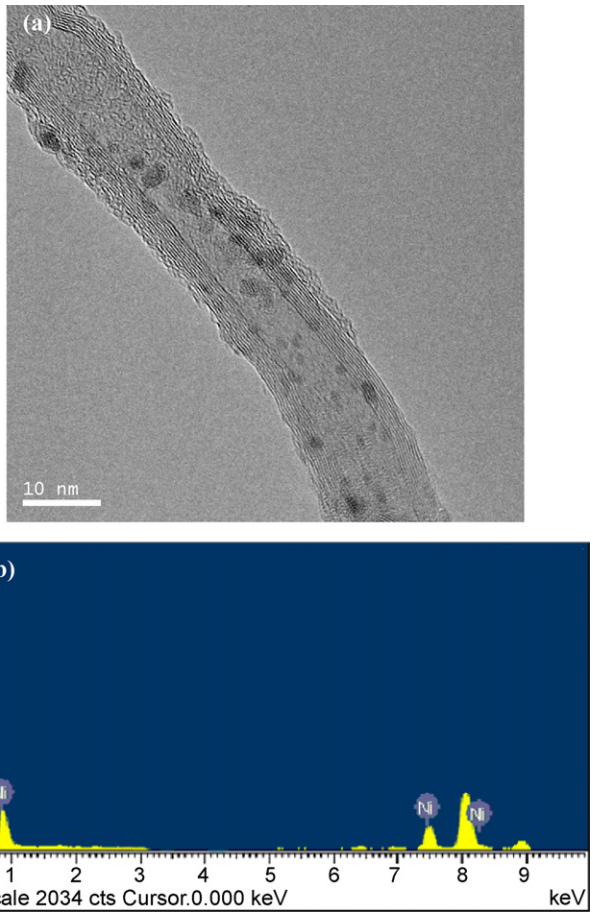

Fig. 3. (a) HR-TEM image of a CNT with EN decoration at 5 °C for 5 min and (b) the corresponding EDS result of the Ni-decorated CNT.

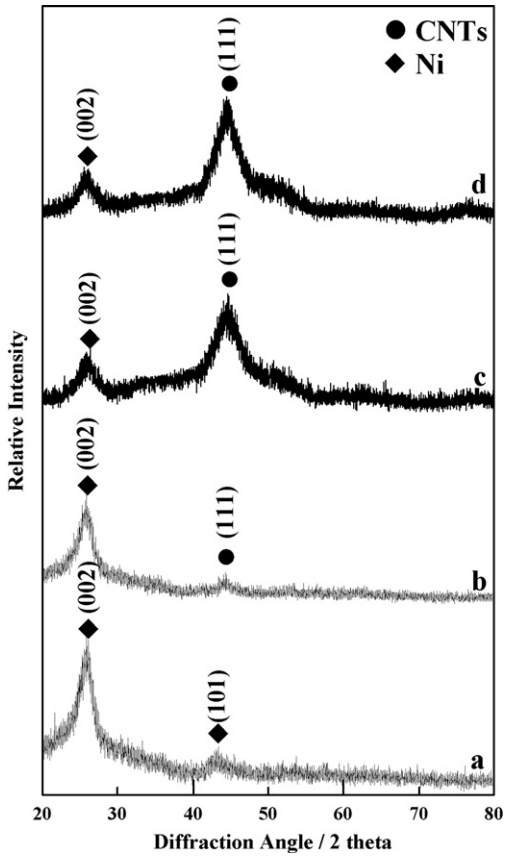

Fig. 2. XRD patterns of (a) as-received CNTs, and those with EN coating at (b) 5 °C for 30 min, (c) 25 °C for 5 min, and (d) 55 °C for 5 min, respectively.

As the deposition temperature was increased to 25 or 55 °C, a drastic increase in Ni particle size was observed. Fig. 6(a) and (b) shows the TEM images for CNTs with EN coating at 25 and 55 °C, respectively, for 5 min. Besides the increase in particle size, the agglomeration of Ni particles also occurs, resulting in clustering of Ni deposits, as demonstrated in Fig. 6. The images revealed in Fig. 6 also indicate that the size distribution of Ni particles was not uniform when EN was conducted at 25 and 55 °C. The existence of extremely large particles suggests that the growth behavior was dominant when EN deposition was performed at a relatively high temperature (>25 °C in this study). Thickening of Ni particle clusters was also observed when the deposition temperature was further increased to 55 °C. By examining the TEM images shown in Figs. 3, 4 and 6, it seems that a uniform distribution of Ni particles on CNTs can be obtained using EN coating, but only at relatively low temperature.

Hydrogen uptake in CNTs with or without Ni decoration was measured using a high-pressure TGA. Hydrogen charging was performed at 28 °C and at a pressure of 6.89 MPa. To avoid the effect of buoyancy of the CNTs under pressure, calibration under He gas

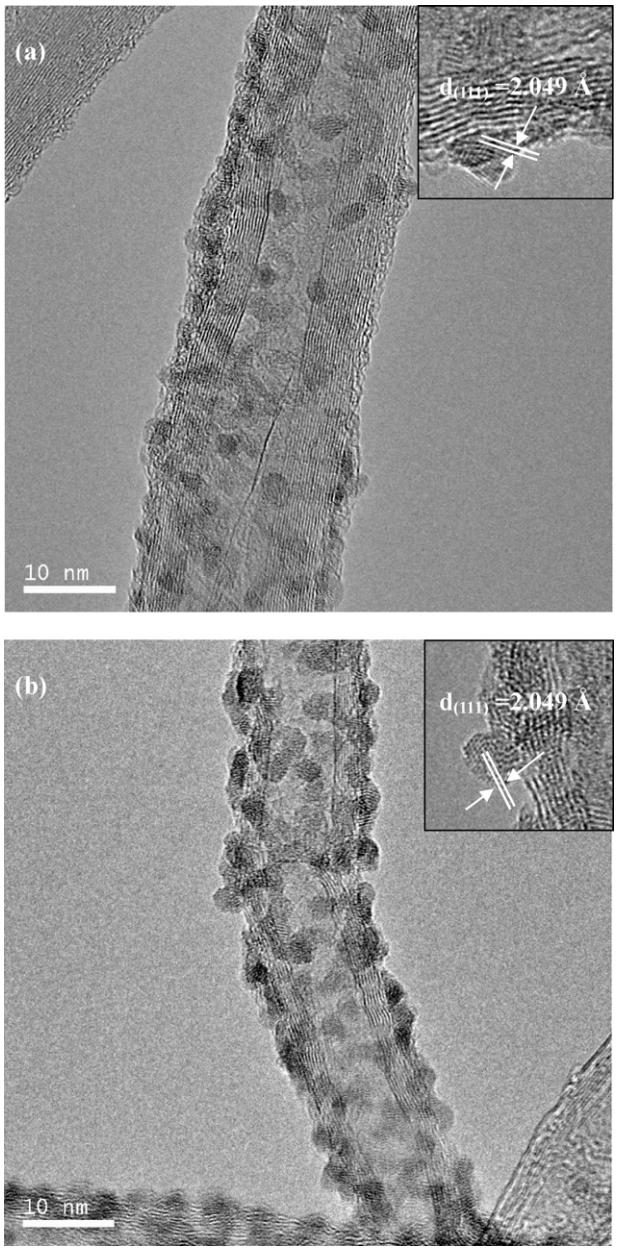

Fig. 4. HR-TEM images of CNTs with EN decoration at 5 °C for (a) 30 min and (b) 60 min.

atmosphere was performed before the weight change measurement of hydrogen uptake. The amount of hydrogen uptake in every charging and discharging cycle was very consistent, indicating the reversibility of hydrogen absorption and desorption processes. The apparent amounts of hydrogen absorbed by CNTs, with and without Ni decoration, are shown in Fig. 7. For the pristine CNTs, the amount of hydrogen absorbed was 0.39 wt.%, consistent with that found in the literature [4]. The hydrogen storage capacity of the activated CNTs, before EN treatment, was 0.32 wt.%, very close to that for pristine CNTs without activation. The residual amounts of Sn and Pd on CNTs after activation treatment were very low, typically 2 and 0.5 wt.%, respectively. The absence of spillover effect of Pd [4,5] was probably because of the negligible amount of its loading on CNTs. With Ni decoration, the amount of hydrogen absorbed increased with increasing Ni content to an optimum level and then decreased afterward. As revealed in Fig. 7, the maximum amount of hydrogen absorbed by Ni-decorated CNTs was 1.14 wt.% when the Ni loading was 10.1 wt.%. Beyond that, the amount of hydrogen stored in the Ni-decorated CNTs decreased. At 25.3 wt.% Ni loading, the amount of hydrogen absorbed was so low that it could not be detected by the high-pressure TGA. The variation of the hydrogen storage capacity of CNTs with different Ni loading is also shown in Table 2. The apparent hydrogen storage capacity shown in Fig. 7 was measured on the basis of the total weight, including CNTs and Ni deposits. Thus, the actual amount of hydrogen absorbed by CNTs could be calculated by subtracting the weight of Ni from the initial weight of the specimen. Since the hydrogen solubility in Ni at 1 and 1000 atm at ambient temperature is about 5.17×10^{-4} and 5.17×10^{-3} wt.%, respectively, and the formation of nickel hydride

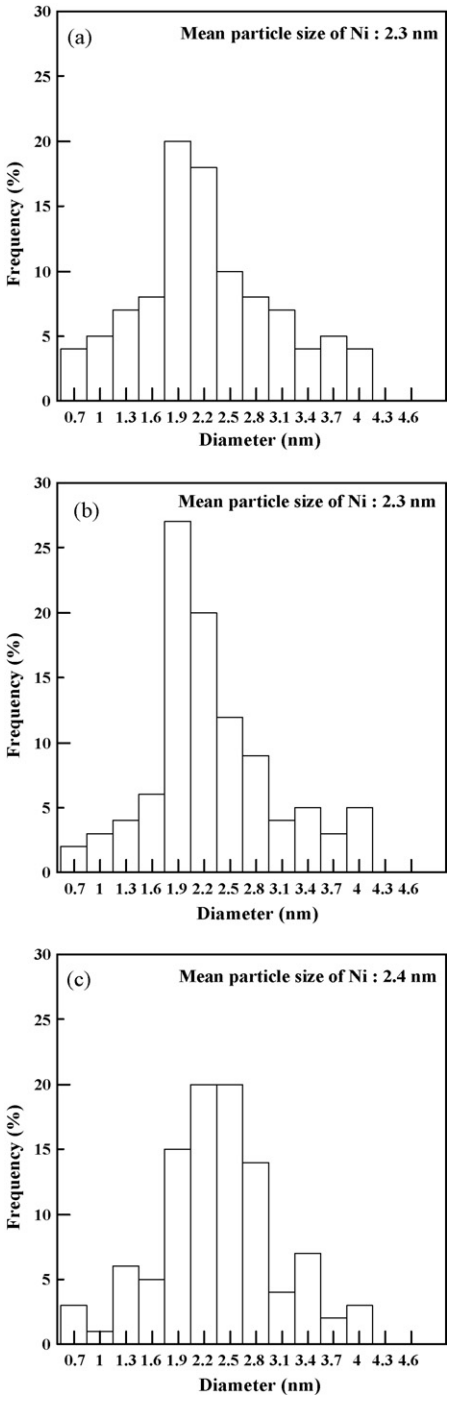

Fig. 5. Histograms of Ni particle size, decorated onto CNTs at 5 °C for (a) 5 min, (b) 30 min, and (c) 60 min.

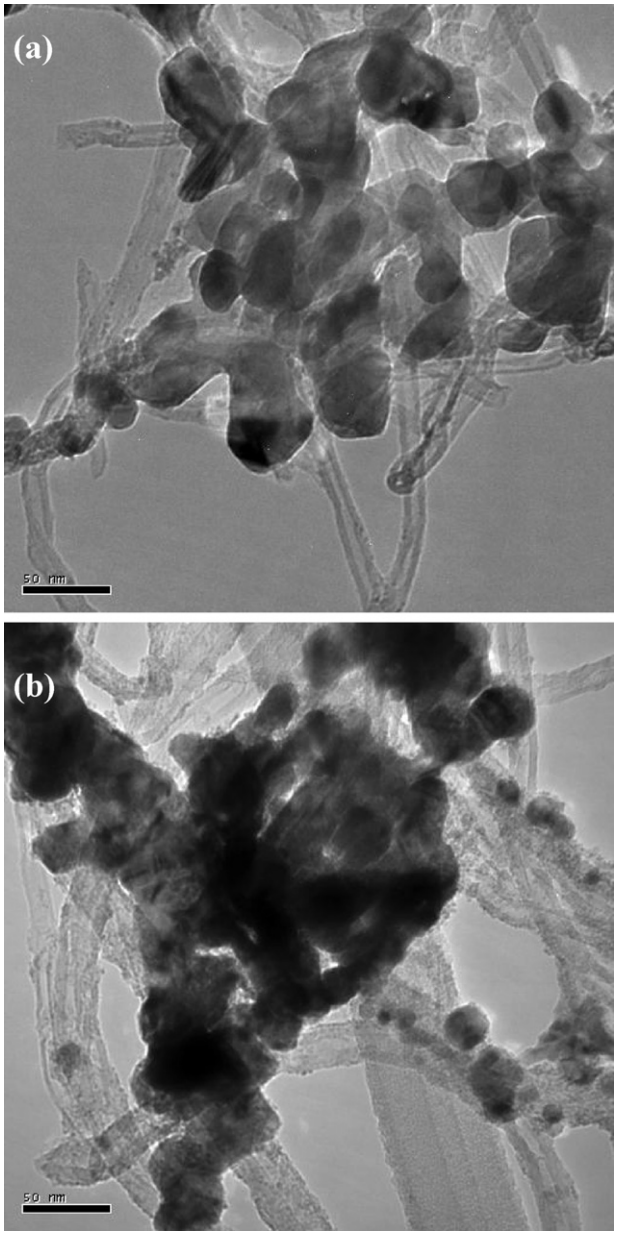

Fig. 6. TEM images of CNTs with EN decoration at (a) 25 °C and (b) 55 °C for 5 min.

is not feasible [24], the amount of hydrogen stored in Ni can be neglected. Thus, the modified hydrogen storage capacity by excluding Ni can be considered as the actual hydrogen storage capacity of CNTs. The modified results are also listed in Table 2. A hydrogen storage capacity of 1.27 wt.%, based on CNTs alone, was obtained for the specimen with 10.1 wt.% of Ni loading, approximately 3 times higher than that without Ni decoration.

Table 2
Hydrogen storage capacity of CNTs with and without Ni decoration.

Sample	Measured hydrogen storage capacity (wt.%)	Modified hydrogen storage capacity (wt.%)
As-received CNTs	0.39	–
CNTs + 3.7 wt.% Ni	0.52	0.54
CNTs + 6.9 wt.% Ni	0.71	0.76
CNTs + 10.1 wt.% Ni	1.14	1.27
CNTs + 15.6 wt.% Ni	0.32	0.38

Measured hydrogen storage capacity = absorbed H_2 (CNTs + absorbed H_2 + Ni)$^{-1}$; modified hydrogen storage capacity = absorbed H_2 (CNTs + absorbed H_2)$^{-1}$.

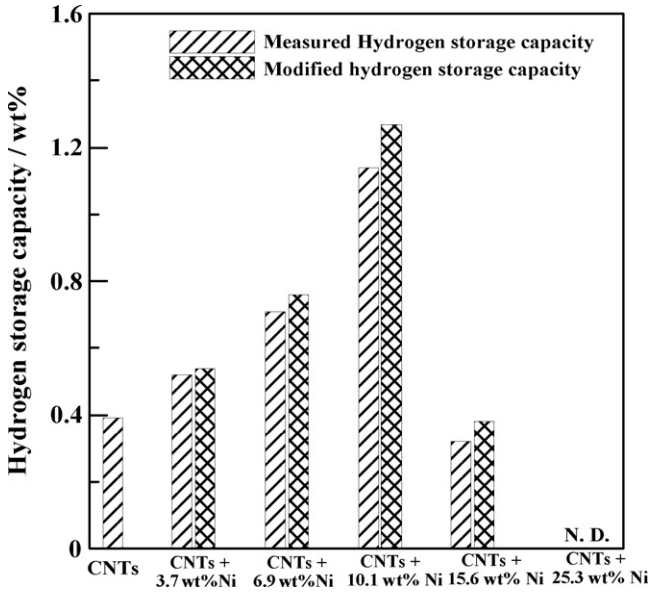

Fig. 7. Hydrogen storage capacity of CNTs with and without Ni decoration.

Without Ni decoration, hydrogen is mainly stored in CNTs by physical adsorption. With the proper amount of Ni deposition on CNTs, an improved hydrogen storage capacity can be obtained, as demonstrated in Fig. 7 and Table 2. The increase in hydrogen uptake may be attributed to the dissociation/spillover effect of the Ni particles deposited on CNTs. The effect of metal catalysts with regard to dissociating hydrogen on support surfaces has long been reported [25]. The most effective metal catalysts for hydrogen spillover are precious metals such as Pt and Pd, although some transition metals, such as Ni and Co, are also useful. With the presence of these catalysts, hydrogen gas can easily dissociate to form hydrogen atoms. The dissociated hydrogen atoms can easily migrate on the support surfaces and subsequently be chemically adsorbed by the sorbents. A substantial increase in hydrogen storage capacity can thus be achieved. Wang and Yang [17] found that Pt and Ru-decoration could cause a significant increase in hydrogen storage capacity for templated carbon or superactivated carbon. The benefits of precious metal decoration with regard to hydrogen uptakes have also been reported for CNTs [10]. However, although Ni-assisted hydrogen uptake has been observed for activated carbon [26], little has been reported for CNTs. Using an impregnation method, Kim et al. [18] found that Ni-decorated CNTs have a higher hydrogen storage capacity than the pristine CNTs. Although electroless Ni deposition to modify the friction and wear properties of CNTs has been investigated, none has been reported for enhancing the hydrogen storage capacity. The results obtained in this investigation indicate that electroless deposited nano-sized Ni particles can indeed improve the hydrogen uptake of CNTs.

As revealed in Fig. 7 and Table 2, the beneficial effect of Ni decoration on hydrogen uptake disappears when the Ni loading exceeds 15.6 wt.%. With excess Ni loading, clustering of Ni particles occurs and the exposed CNT surface area decreases, which subsequently causes a reduction in the active sites for either physical or chemical adsorption. As a result, the hydrogen storage capacity is reduced. At a Ni loading of 25.3 wt.%, hydrogen uptake cannot even be measured. In contrast, the beneficial effect of Ni decoration on hydrogen uptake is observed when Ni loading is lower than 10.1 wt.%. From the TEM images shown in Figs. 3 and 4, discrete nano-sized Ni particles are uniformly distributed onto CNTs. These results indicate that the benefit of hydrogen gas dissociation/spillover reaction with regard to Ni particles depends on their distribution on the surface of CNTs. An optimum effect is observed when a higher density

and uniformly distributed nano-sized Ni particles are formed. The importance of catalyst distribution on improving hydrogen storage capacity has also been found for the Ni- and Pd-decorated CNTs, as reported elsewhere [27]. Since the reversibility of hydrogen uptake is very important in practical use, whether Ni decoration can also assist the release of chemisorbed hydrogen in CNTs, especially at ambient temperature is of great concern and needs further investigation.

4. Conclusions

Ni decoration onto CNTs can be successfully performed by employing an EN process. Specifically, uniform distribution of Ni particles on CNTs can be obtained by applying EN at 5 °C, with the density of deposited particles increasing with the deposition time. The mean particle size was about 2.3 nm when Ni was deposited at 5 °C. At temperature higher than 25 °C, the deposition rate was very fast and clustering of Ni particles was observed.

The amount of hydrogen absorbed by Ni-decorated CNTs increased with increasing Ni loading up to a maximum of 1.24 wt.%, about 3 times higher than that of the pristine CNTs. The enhanced hydrogen absorption was attributed to the spillover effect provided by the nano-sized Ni particles which were uniformly distributed on CNTs. The beneficial effect of Ni decoration on hydrogen uptake decreased when Ni loading exceeded 15.6 wt.%, and even disappeared at a Ni loading of 25.3 wt.%, probably due to blocking of the active sites for either physical or chemical adsorption of hydrogen.

Acknowledgement

The authors would like to thank the National Science Council of the Republic of China for financial support of this research under Contract No. NSC 96-2221-E-006-006.

References

[1] F.L. Darkrim, P. Malbrunot, G.P. Tartaglia, Int. J. Hydrogen Energy 27 (2002) 193–202.
[2] B. Panella, M. Hirscher, S. Roth, Carbon 43 (2005) 2209–2214.
[3] M. Hirscher, B. Panella, J. Alloy Compd. 404 (2005) 399–401.
[4] A.D. Lueking, R.T. Yang, J. Catal. 206 (2002) 165–168.
[5] A.D. Lueking, R.T. Yang, Appl. Catal. A 265 (2004) 259–268.
[6] Y. Suttisawat, P. Rangsunvigit, B. Kitiyanan, M. Williams, P. Ndungu, M.V. Lototskyy, A. Nechaec, V. Linkov, S. Kulprathipanja, Int. J. Hydrogen Energy 34 (2009) 6669–6675.
[7] S. Kocabas, T. Pokac, G. Dogu, T. Dogy, Int. J. Hydrogen Energy 33 (2008) 1693–1699.
[8] S.C. Mu, H.L. Tang, S.H. Qian, M. Pan, R.Z. Yuan, Carbon 44 (2006) 762–767.
[9] C.H. Chen, C.C. Huang, Micropor. Mesopor. Mater. 109 (2008) 549–559.
[10] J.W. Lee, H.S. Kim, J.Y. Lee, J.K. Kang, Appl. Phys. Lett. 88 (2006) 143126–143129.
[11] G.G. Wildgoose, C.E. Banks, R.G. Compton, Small 2 (2006) 182–193.
[12] X.H. Peng, J.Y. Chen, J.A. Misewich, S.S. Wang, Chem. Soc. Rev. 38 (2009) 1076–1098.
[13] S. Arai, M. Endo, N. Kaneko, Carbon 42 (2004) 641–644.
[14] C. Bittencourt, A. Felten, J. Ghijesen, J.J. Pireaux, W. Drube, R. Erni, G.V. Tendeloo, Chem. Phys. Lett. 436 (2007) 368–372.
[15] S. Rather, R. Zacharia, S.W. Hwang, M. Naik, K.S. Nahm, Chem. Phys. Lett. 441 (2007) 261–267.
[16] F. Wang, S. Arai, K.C. Park, K. Takeuchi, Y.J. Kim, M. Endo, Carbon 44 (2006) 1307–1310.
[17] L. Wang, R.T. Yang, J. Phys. Chem. C 112 (2008) 12486–12494.
[18] H.S. Kim, H. Lee, K.S. Han, J.H. Kim, M.S. Song, M.S. Park, J.Y. Lee, J.K. Kang, J. Phys. Chem. B 109 (2005) 8983–8986.
[19] W. Li, C. Liang, W. Zhou, J. Qiu, Z. Zhou, G. Sun, Q. Xin, J. Phys. Chem. B 107 (2003) 6292–6299.
[20] X. Li, H. Zhu, C. Xu, Z. Mo, D. Wu, Int. J. Hydrogen Energy 28 (2003) 1251–1253.
[21] W. Pan, X. Zhang, S. Li, D. Wu, Z. Mo, Int. J. Hydrogen Energy 30 (2005) 719–722.
[22] L.M. Ang, T.S.A. Hor, G.Q. Xu, C.H. Tung, S.P. Zhao, J.L.S. Wang, Carbon 38 (2000) 363–372.
[23] Y. Du, H. Chen, R. Chen, N. Xu, Appl. Catal. A 277 (2004) 259–264.
[24] T.B. Massalski, O. Hiroaki, Binary Alloy Phase Diagrams, ASM, Ohio, 1990.
[25] A.J. Robell, E.V. Ballou, M. Budart, J. Phys. Chem. 68 (1964) 2748–2753.
[26] M. Zielinski, R. Wojcieszak, S. Monteverdi, M. Mercy, M.M. Bettahar, Catal. Commun. 6 (2005) 777–783.
[27] C.Y. Chen, J.K. Chang, K.Y. Lin, S.T. Chung, W.T. Tsai, Mater. Sci. Forum 638 (2010) 1148–1151.